JOURNAL OF THEORETICAL AND APPLIED MECHANICS
62, 3, pp. 521-534, Warsaw 2024
https://doi.org/10.15632/jtam-pl/189805

FEED-FORWARD ARTIFICIAL NEURAL NETWORK AS SURROGATE MODEL TO PREDICT LIFT AND DRAG COEFFICIENT OF NACA AIRFOIL AND SEARCHING OF MAXIMUM LIFT-TO-DRAG RATIO

Rafał Kieszek, Maciej Majcher, Borys Syta, Adam Kozakiewicz
Military University of Technology, Faculty of Mechatronics, Armament and Aerospace, Warsaw, Poland
e-mail: borys.syta@wat.edu.pl

The problem of computation time in numerical calculations of aerodynamics has been studied by many research centres. In this work, a feed forward artificial neural network (FF-ANN) was used to determine the dependence of lift and drag coefficients on the angle of attack for NACA four-digit families. A panel method was used to generate the data needed to train the FF-ANNs. Optimisation using a genetic algorithm and a neural metamodel resulted in a non-standard NACA aerofoil for which the optimal angle of attack was determined with a maximum L/D ratio. The optimisation results were validated using the finite volume method.

Keywords: Artificial Neural Network (ANN), NACA airfoil, optimization, surrogate model, model reduction

List of designations

α – angle of attack
C_l, C_d – lift and drag coefficient, respectively
K – lift-to-drag ratio, L/D ratio
m – maximum camber in tenths of chord
p – position of the maximum camber along chord in tenths of chord
R – regression
R^2 – coefficient of determination
t – maximum airfoil thickness in tenths of chord
x_U, x_L, y_U, y_L – coordinates of point for upper (U) and lower (L) edge of airfoil
y_t, y_c – thickness and camber coordinates, respectively
θ – angle of inclination of tangent to chamber of airfoil at point
Ma_H – Mach number of undisturbed flow

1. State of the art

The use of artificial intelligence in engineering is becoming increasingly popular. The main task of artificial intelligence research is to construct machines and computer programs capable of performing selected functions of the mind and human senses, not amenable to numerical algorithmization. Such problems are sometimes called AI-complete and include decision-making in the absence of all data. This paper uses AI to predict behavior of a system for intermediate values not present in the results of numerical simulations.

The applications of Artificial Neural Networks (ANNs) is becoming increasingly popular, especially in areas that require time-consuming numerical calculations. One such an area is aerodynamic analysis. Costly wind tunnel tests or time-consuming CFD (computational fluid dynamics) analyses are required to determine aerodynamic characteristics of aerofoils. In this paper, the authors propose an alternative approach by replacing hard calculations (like CFD) with ANNs. The objective of this work was to demonstrate that this approach could enable rapid analysis of aerofoils and determine their aerodynamic characteristics without the need to perform numerical analyses for each aerofoil in a selected family of NACA aerofoils.

The problem of computation time for numerical calculations of aerodynamics has been studied by many research centres all over the world, demonstrating its complexity and the need for novel solutions. A variety of methods have been used to reduce the running time of algorithms. For example, Proper Orthogonal Decomposition (POD) (Berkooz *et al.*, 1992) is a method that reduces complexity of numerical simulations, such as CFD. Typically, it is used in CFD analyses (including turbulence analyses) to replace the Navier-Stokes equations with models that are simpler to solve. This method has been used by Bakewell and Lumley (1967), among others. Various methods based on machine learning tied to CFD are used to reduce computation time (San and Maulik, 2018), usually combined with neural networks. However, an ANN requires a large volume of training data and thus significant computational time. This problem was presented by Fukami *et al.* (2021). Buterweck and Głuch (2014) used ANNs to analyse the effect of Mach number on the prediction of turbine blade degradation. Prediction of aerodynamic characteristics using an artificial neural network for a wind turbine was performed by Verma and Baloni (2021). Sekar *et al.* (2010) presents an approach based on analysis of data produced with a CFD solver to predict the incompressible laminar flow field around aerofoils. The approach was based on a combination of a deep convolutional neural network (CNN) and a deep multilayer perceptron (MLP). Aramendia *et al.* (2019) used ANNs to predict the aerodynamic efficiency of Gurney flaps. A CFD-based drag coefficient analysis was also carried out in (Viquerat and Hachem, 2020), where a set of random geometries based on Bézier curves was prepared to train the neural network. Pressure distributions were calculated for several representative cases. In addition, a lift and drag coefficient was predicted based on CFD approximation calculations (Kharal and Saleem, 2012). Kharal and Saleem (2012) described an aerofoil using Bézier curves, developed their aerodynamic characteristics and then proceeded with FF-ANN training. The inverted ANNs were then used to determine aerofoil geometry for a given drag coefficient. Similarly, inverted ANNs were used in (Sun *et al.*, 2015), where geometry of the aerofoil was described as shown in Fig. 1. The pressure distribution on the aerofoil and then on the wing was determined by the proposed ANN algorithm. Thirumalainambi and Bardina (2003) also analysed the optimal ANN structure for predicting aerodynamic coefficients of an aircraft.

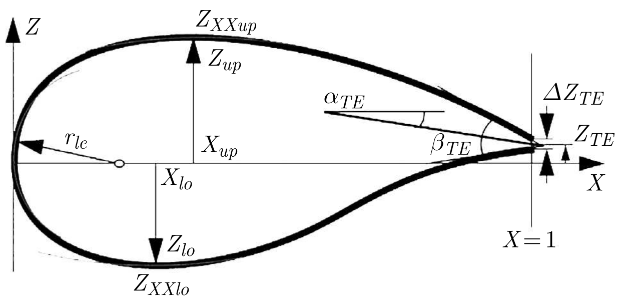

Fig. 1. Airfoil geometry (Sobieczky, 1999)

A frequently used method for optimising aerodynamics is genetic algorithms. Porta Ko *et al.* (2023) describes the process of optimising kinked aerofoils using the NSGA-II (Non-dominated

Sorting Genetic Algorithm). Optimisation to minimise the aerodynamic forces generated was carried out in (Khan *et al.*, 2022) where solar panels were studied.

The most common method used in computer fluid mechanics is the finite volume method (FVM) used for CFD analyses, which takes place in conjunction with ANNs. One example of less commonly used methods would be a combination of the vortex method and a neural network (Sessarego *et al.*, 2020).

The use of surrogate models is relatively infrequently used in practice due to errors arising from the surrogate model approximations. The main purpose of the article is to demonstrate that it is possible to prepare a surrogate model based on AI or, more precisely, SSN. The accuracy of such a model should be sufficient and the optimization results should be no worse than the available solutions.

2. NACA four-digit family

In this work, an artificial neural network was used to determine the dependence of lift and drag coefficients on the angle of attack for NACA four-digit aerofoils. First, the data was generated from an open database of aerodynamic diagrams to train the ANN. The data generation was described by Drela (1989).

An asymmetric NACA four-digit aerofoil (NACA – National Advisory Committee for Aeronautics, NACAmpt) is defined by three parameters: m, p, t. Equations (2.1) and (2.2) were used to describe the aerofoil geometry mathematically, based on the work [12]

$$\begin{aligned} x_U &= x - y_t \sin\theta \qquad & y_U &= y_c + y_t \cos\theta \\ x_L &= x + y_t \sin\theta \qquad & y_L &= y_c - y_t \cos\theta \end{aligned} \tag{2.1}$$

and

$$\begin{aligned} y_t &= \pm\frac{t}{0.2}(a_1\sqrt{x} - a_2x - a_3x^2 + a_4x^3 - a_5x^4) \\ \theta &= \arctan\frac{dy_c}{dx} \\ y_c &= \begin{cases} \dfrac{m}{p^2}(2px - x^2) & \text{for} \quad 0 \leqslant x \leqslant p \\ \dfrac{m}{(1-p)^2}[(1-2p) + 2px - x^2] & \text{for} \quad p \leqslant x \leqslant 1 \end{cases} \end{aligned} \tag{2.2}$$

where: $a_1 = 0.2969$, $a_2 = 0.1260$, $a_3 = 0.3516$, $a_4 = 0.2843$, $a_5 = 0.1015$ – coefficients defined by NACA.

In the remainder of this work, only asymmetrical aerofoils were analysed. The database of aerodynamic coefficients acting on the aerofoil was determined with reference to (Oliveira, 2021), where after a simple parameterisation of the code, the lift C_l and drag C_d versus the angle of attack α was calculated by Xfoil. Xfoil is a panel-based software that enables analysis of aerofoils and wings operating at low Reynolds numbers.

3. Artificial neural network

This paper uses a feed-forward artificial neural network (FF-ANN). The input (training) parameters for the NACA aerofoil number were: $m, p \in \langle 2; 8\rangle$, $t \in \langle 8; 24\rangle$, as well as angles of attack α within $\pm 24°$. The output (training) data was determined using the Xfoil software; the lift and drag coefficients corresponding to the cases in the input database. The Reynolds number $\mathrm{Re} = 5.7 \cdot 10^6$ and Mach number $\mathrm{Ma}_H = 0.1439$ were set as constant values. This corresponded to velocity of 49.39 m/s for an average aerodynamic chord of length 1.738 m. The database containing the characteristics of 441 profiles was needed to train the artificial neural network. Due to the lack of availability of such a large database of NACA four-digit profiles, it was decided to use Xfoil to prepare it.

As a result of numerical analyses, it was decided to develop separate ANNs (trained in parallel) for the prediction of lift and drag coefficients for selected angles of attack from the range $\pm 24°$ with an increment of $\Delta\alpha = 2°$.

The MATLAB Neural Network Toolbox was used as the ANN environment. The ANNs were trained using the SCG (Scaled Conjugate Gradient) backpropagation algorithm. The objective of the training was to minimise the mean squared error (MSE) of the data fit. The ANN architecture was optimised, where the mean absolute error (MAE) was the objective function. An optimisation of the ANN structure using a genetic algorithm was done for two and three hidden layers. A feed-forward ANN (3-65-8-1) was chosen as the optimal ANN structure. A diagram of the ANN used is shown in Fig. 2. The optimisation was run until MAE was no greater than 3%. During the ANN optimisation, the size of the ANN was not increased beyond 500 neurons to prevent "learning by heart".

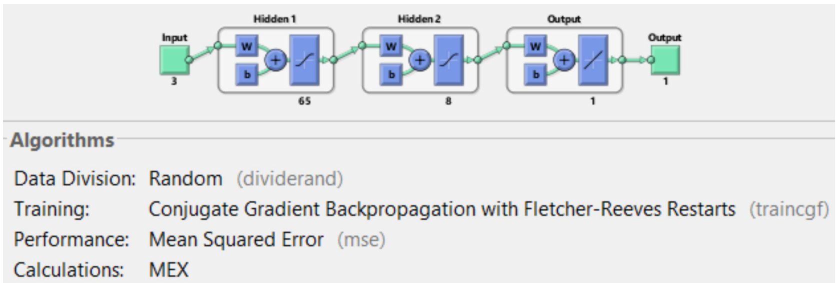

Fig. 2. Scheme of the used artificial neural network, where: w – weights, b – bias

Figure 3 shows the regression results for the ANNs used, trained for the zero angle of attack and the predicted values of the drag coefficient C_d. A high regression coefficient of $R = 0.9858$ was obtained for all the data.

A separate ANN was used for each angle of attack. This reduced the duration of the learning process and increased the accuracy of the ANN learning. The learning time for all optimised ANNs was less than 130 seconds with an approximation error less than 1%. Figure 4 shows the coefficient of lift C_l and drag C_d predicted by the trained ANNs, as a function of the angle of attack for the NACA 2412 aerofoil. The neural model achieved a high coefficient of determination for both lift (0.9984) and drag coefficient prediction (0.9911), compared to the data generated with Xfoil. It also presents the lift and drag coefficients obtained in experimental tests, based on a NACA report (Abbott *et al.*, 1945). For angles of attack from $-10°$ to $16°$, the analysis performed with Xfoil and ANN were consistent with experimental tests. For larger angles, the differences were significant. This could be due to the choice of the Reynolds number in the Xfoil software, as confirmed by the conclusions from (Günel *et al.*, 2016) or a tendency towards numerical errors for angles of attack: $\alpha > 8°$ (Saad *et al.*, 2017). However, in order to determine the aerofoil L/D ratio, the accuracy of the ANN was sufficient, as usually the maximum L/D ratio corresponds to an angle of attack in the range from $2°$ to $8°$.

In order to test the adopted research concept, the lift coefficient as a function of angle of attack was calculated for a non-standard NACA four-digit aerofoil in Xfoil. This aerofoil was not present in the ANN teaching database. This aerofoil was NACA model (2.4)(3.6)12, where $m = 2.4$, $p = 3.6$ and $t = 12$ are shown in Fig. 5, which was numerically analysed using the panel method. Comparative results for the Xfoil and ANN are shown in Fig. 6.

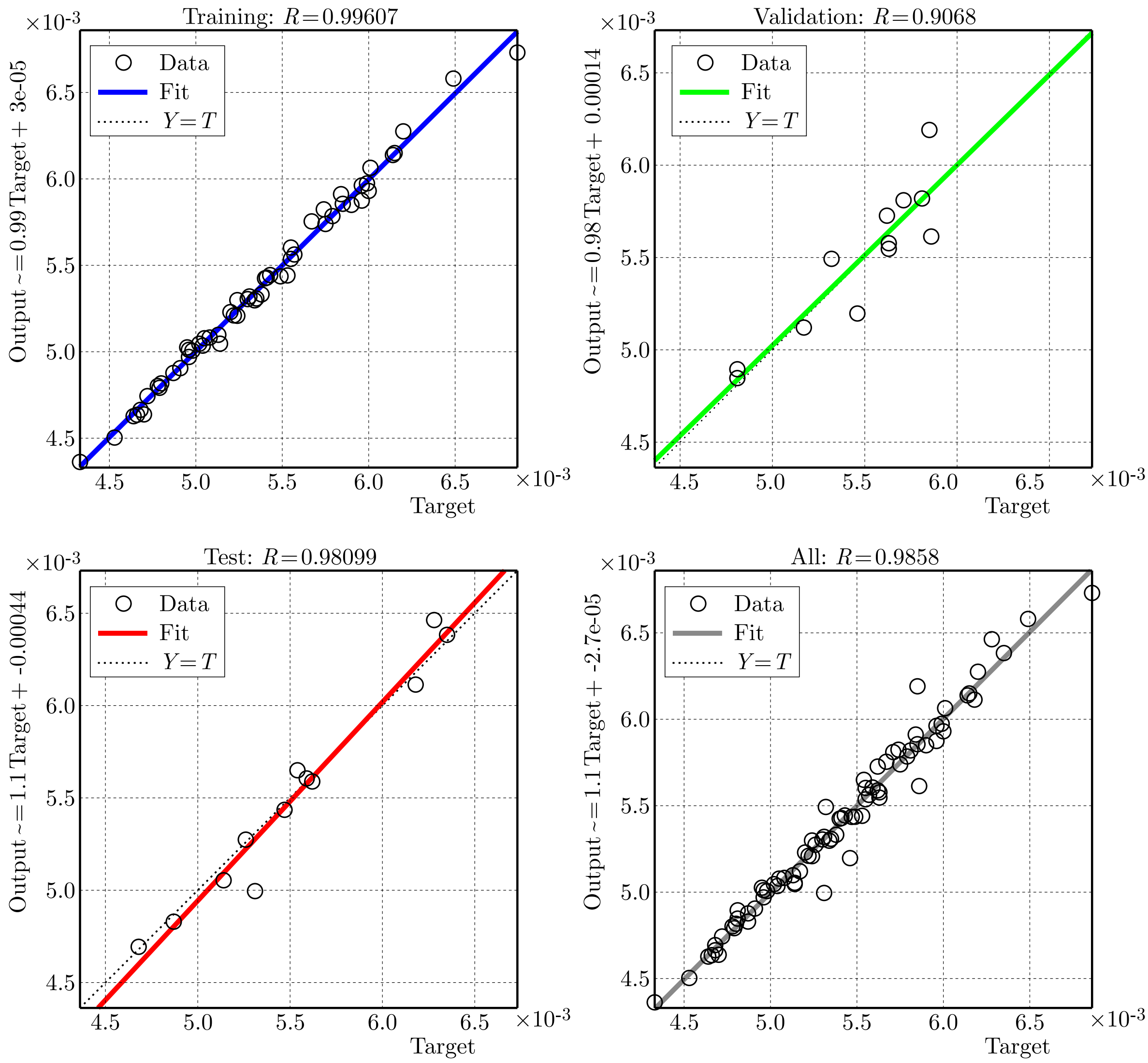

Fig. 3. Regression of used ANN

For the NACA (2.4)(3.6)12 aerofoil, the coefficient of determination (R^2) of the lift coefficient was 0.998. However, the ANN was not able to correctly predict the distribution of the drag coefficient for larger angles of attack (above 16° and below −10°). For angles of attack between −10° and 16°, the accuracy was higher, and the corresponding coefficient of determination was 0.9942, as shown in Fig. 7.

4. Optimization

In this work, an attempt at optimisation was made using the presented neural metamodel to maximise the L/D ratio, $K = C_l/C_x$. Both the lift and drag coefficients were determined using ANNs. The default genetic algorithm (GA) in Matlab was used for optimisation, the working principle of which was based on (Conn *et al.*, 1991). In the algorithm used, the decision variables were parameters m, p and t, which described geometry of the aerofoil. Restrictive conditions related to the span of the database that were used to teach the ANN were imposed, assuming that m = 2-6, p = 2-6 and t = 12-24. The angle of attack α was a discrete variable within ±24° with an increment of 2°. The algorithm with the objective function determined the aerofoil L/D ratio K for all angles of attack α and returned its largest value, the corresponding angle

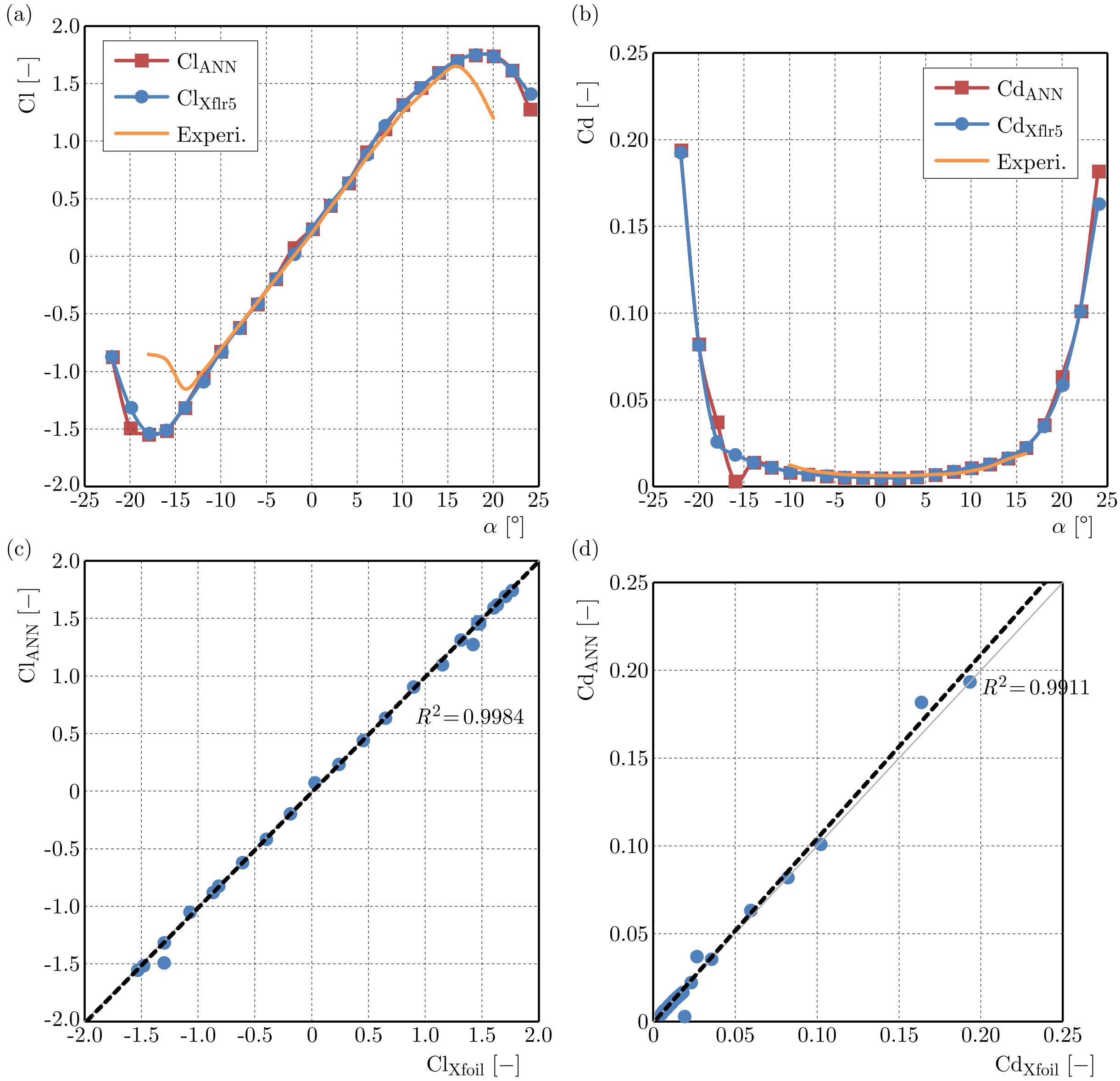

Fig. 4. Predicted, computed and by Xfoil experimental lift (a) and drag (b) coefficients vs. the angle of attack, and the coefficient of determination of lift (c) and drag (d) coefficients for NACA 2412

of attack and the values of the decision variables defining the aerofoil geometries. The NACA 12(5.18)(4.18) aerofoil resulting from the optimisation is shown in Fig. 8.

According to the ANN, the maximum L/D ratio of the tested aerofoil corresponded to the angle of attack $\alpha = 4°$, and after optimisation it was $K = 194.4$ for the ANN and $K = 197.4$ for Xfoil. This provided the difference of relative error of L/D ratio $RE(K) = 1.53\%$. Figure 9 shows the relationship $RE(K) = f(\alpha)$. For angles of attack below $\alpha = -12°$, the calculations diverged.

Thinner aerofoils achieved higher L/D ratios, so the algorithm naturally brought the aerofoil thickness down to a lower limit $t = 12$. Due to simplifications made for the drag coefficient confounded in the Xfoil software, a comparative analysis of the prediction results from the ANN, the Xfoil programme and the Ansys Fluent software were applied.

For further numerical tests of the aerofoil after the optimisation process, a suitable geometrical model of the aerofoil was developed, together with the computational domain in the Ansys Workbench DesignModeler software (Fig. 10).

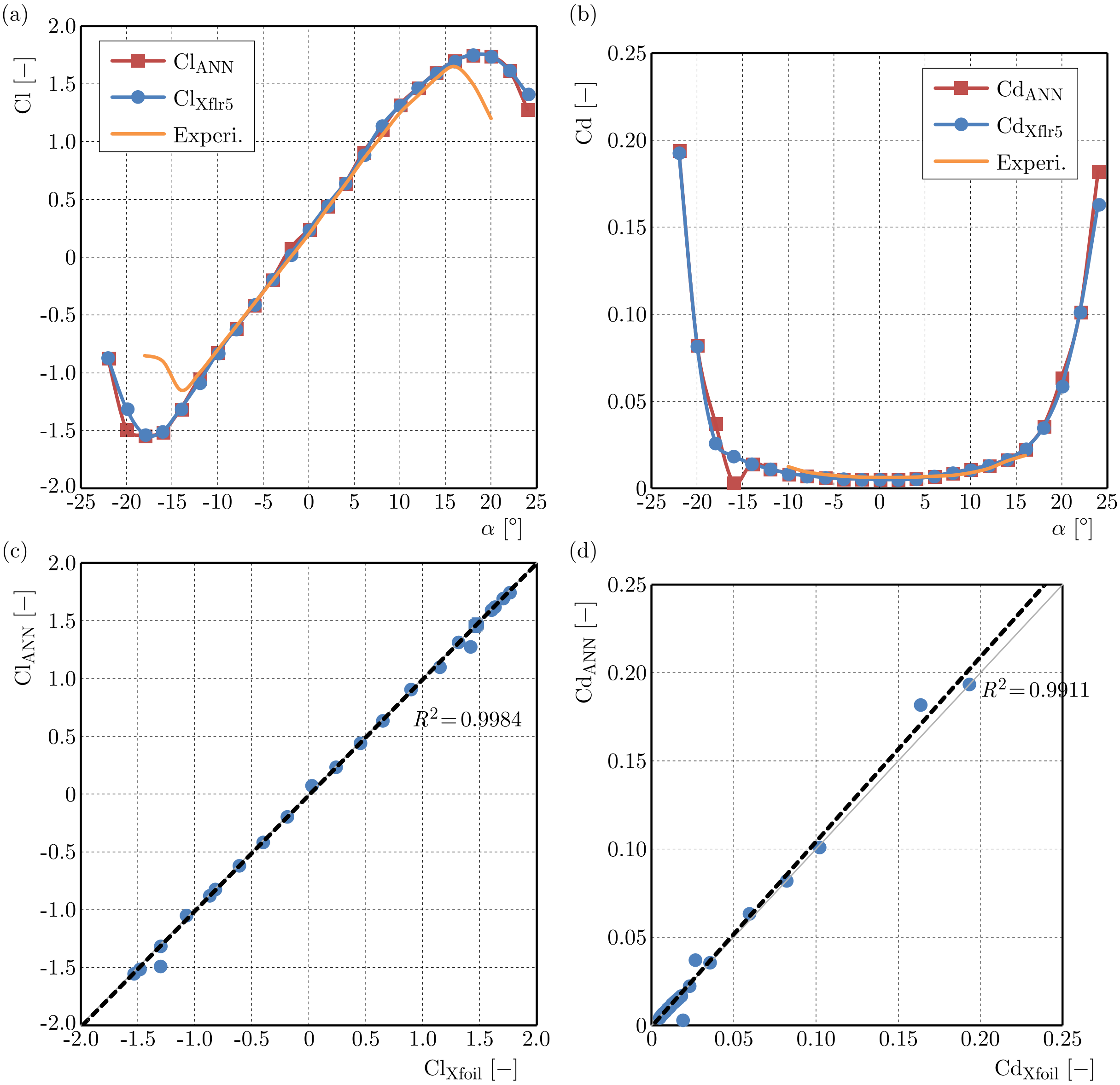

Fig. 5. Example of geometry of a non-standard NACA aerofoil (2.4)(3.6)12

At the stage of developing the domain for digitisation, the relevant edges were assigned with appropriate names representing the boundary conditions. The outer edges of the calculation area were assigned with a pressure-far-field condition, while the edges representing the aerofoil outline were assigned with a wall condition. The computational area was then digitised. The developed computational domain was digitised using a structured grid (Fig. 10a). The grid was appropriately compacted towards the aerofoil (Fig. 10b). The total number of grid elements was 306 000. The numerical grid thus developed was exported in .msh format to Ansys Fluent for numerical simulations of the flow around the aerofoil.

Numerical flow simulations were performed for the Mach number $\mathrm{Ma}_H = 0.1439$ and a reference pressure of 101325 Pa, with Double Precision and Density-Based solver settings (the "Implicit" method). Numerical simulations of the flow around the aerofoil were done over a range of angles of attack $\alpha = \pm 24°$ with an increment of $\Delta\alpha = 2°$. The determinant of convergence of the calculations, and thus the termination of simulation for a given angle of attack, was the obtained value – which was constant in the iteration function of the lift and drag coefficients referenced to the value of the chord, 1.738 m.

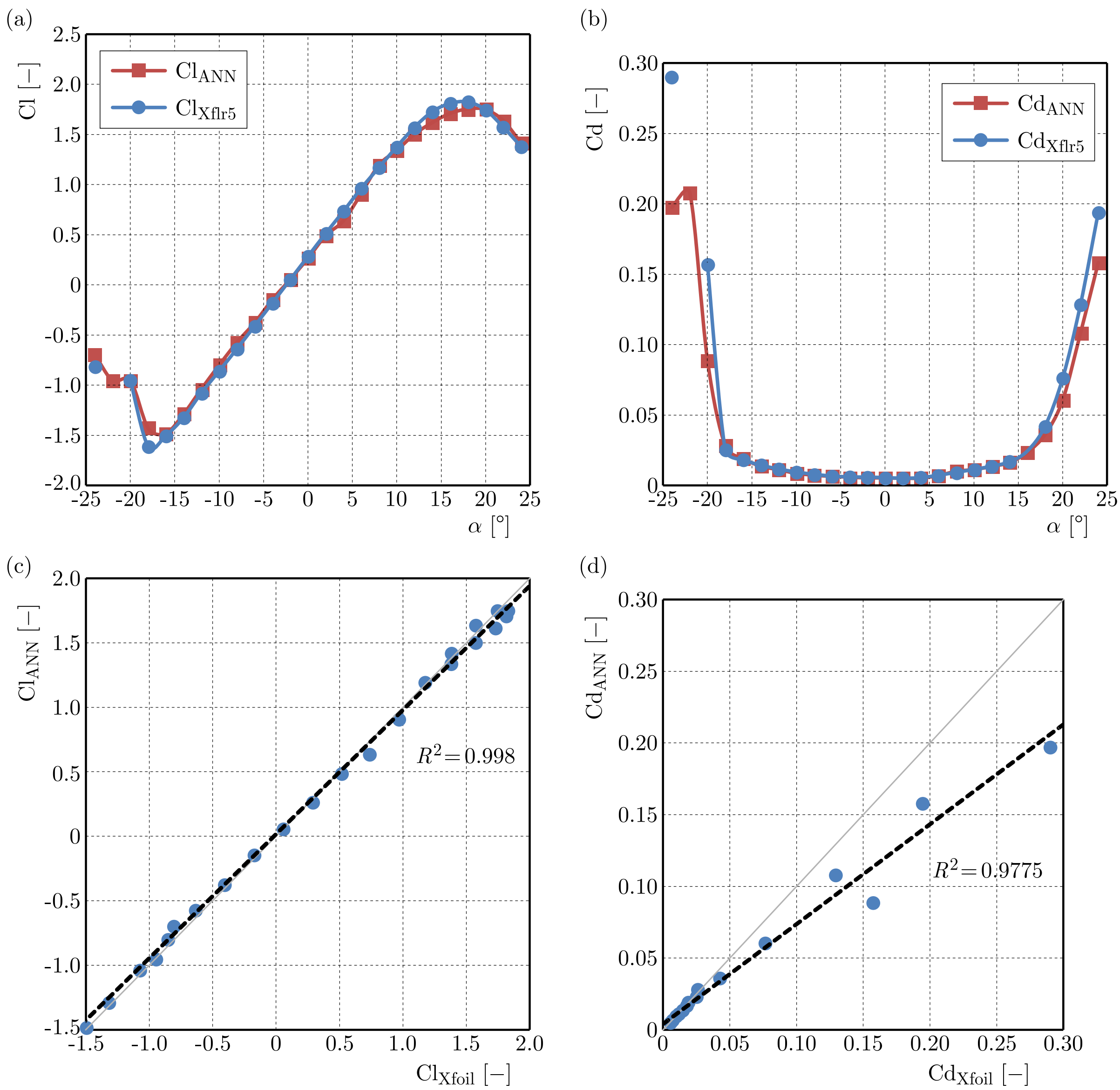

Fig. 6. Predicted by SSN and computed by Xfoil (Xflr5) lift (a) and drag (b) coefficients vs. the angle of attack, and the coefficient of determination of lift (c) and drag (d) coefficients for NACA (2.4)(3.6)12

The results of analyses comparing the aerodynamic characteristics of the optimised aerofoil obtained with the ANN, Xfoil and Ansys Fluent are shown in Fig. 11.

Based on the obtained characteristics, it can be concluded that a satisfactory agreement was achieved, especially in the linear range $C_l = f(\alpha)$. Over the range of critical angles of attack, the lift coefficients obtained from the calculations performed in Ansys Fluent and Xfoil were very close to each other, and partly differed from the values obtained based on the ANN prediction. A similar situation occurred with large negative angles of attack $-15°$ to $-24°$. In the case of the $C_d = f(\alpha)$ characteristics, the drag force coefficients obtained from the numerical analyses run in the Ansys Fluent software were higher than the values obtained from the ANN prediction and Xfoil calculations. This is because for each angle of attack, the Ansys Fluent software determined the drag as the sum of the pressure drag and friction drag. In the case of SSN and Xfoil, the drag calculations run with the assumption of constant freestream velocity and the steady flow which resulted in increased inaccuracies at higher angles of attack. As with the previous profile, the ANN prediction for the drag coefficient over the full range of angles of attack was inadequate. However, for the angles of attack in the range from $-10°$ to $14°$, it was already higher, and the coefficient of determination was $R^2 = 0.9983$, as shown in Fig. 12.

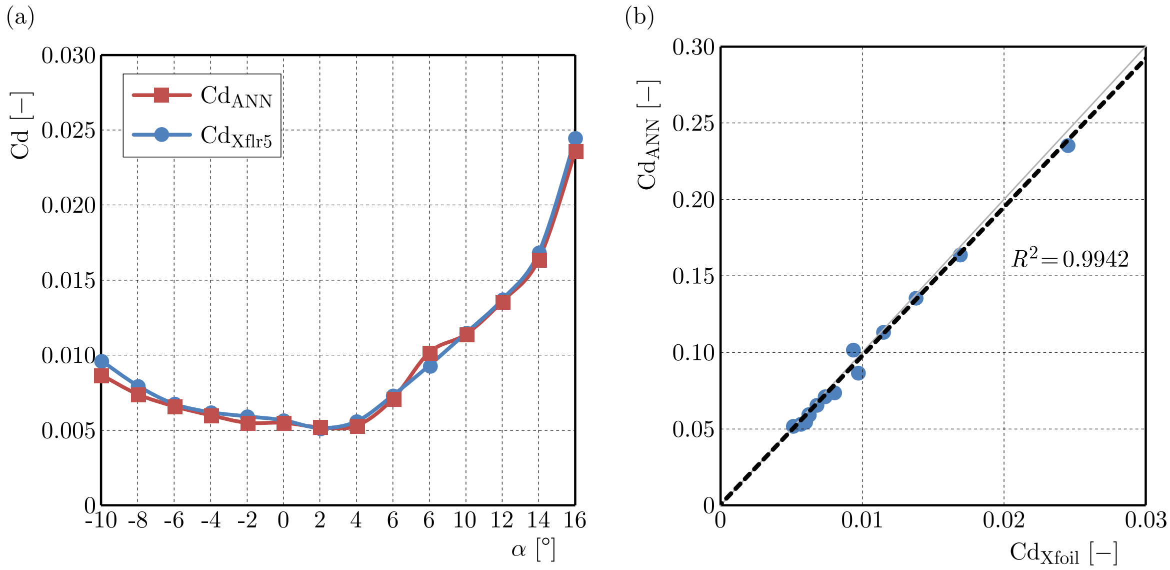

Fig. 7. Predicted by SSN and computed by Xfoil drag coefficients vs. the angle of attack (a) and the coefficient of determination of the drag coefficient (b) for small angles of attacks ($-10 \leqslant \alpha \leqslant 16°$) for NACA (2.4)(3.6)12

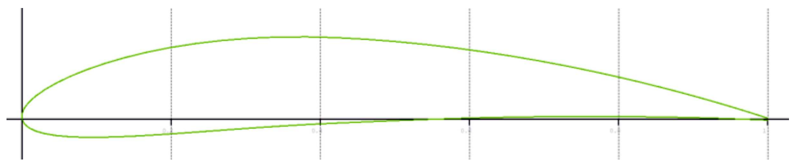

Fig. 8. NACA 12(5.18)(4.18) aerofoil, a result of the optimisation algorithm

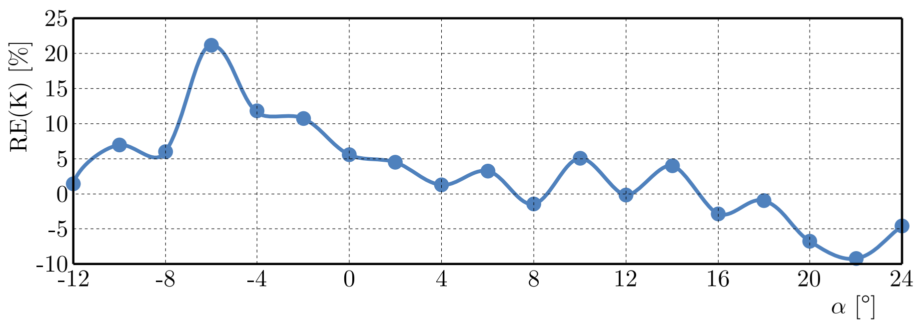

Fig. 9. Relative difference in the L/D ratio determined by ANN and Xfoil

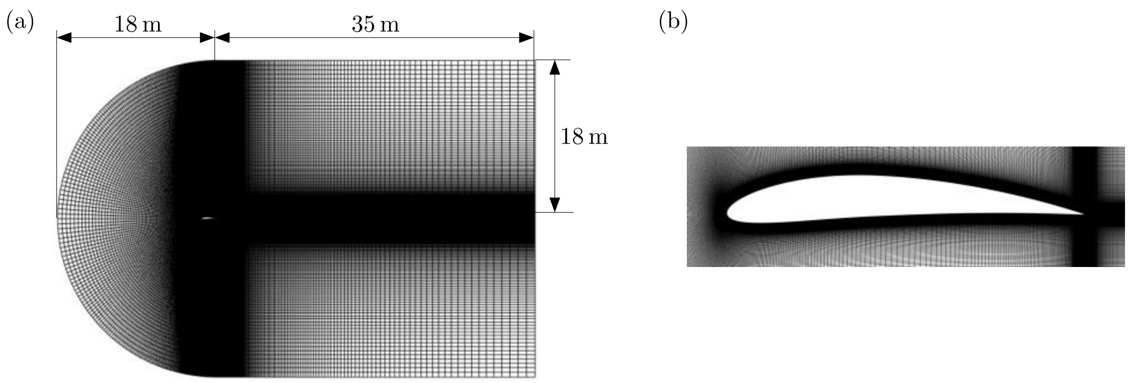

Fig. 10. Discretized computational domain (a), discretized airfoil area (b)

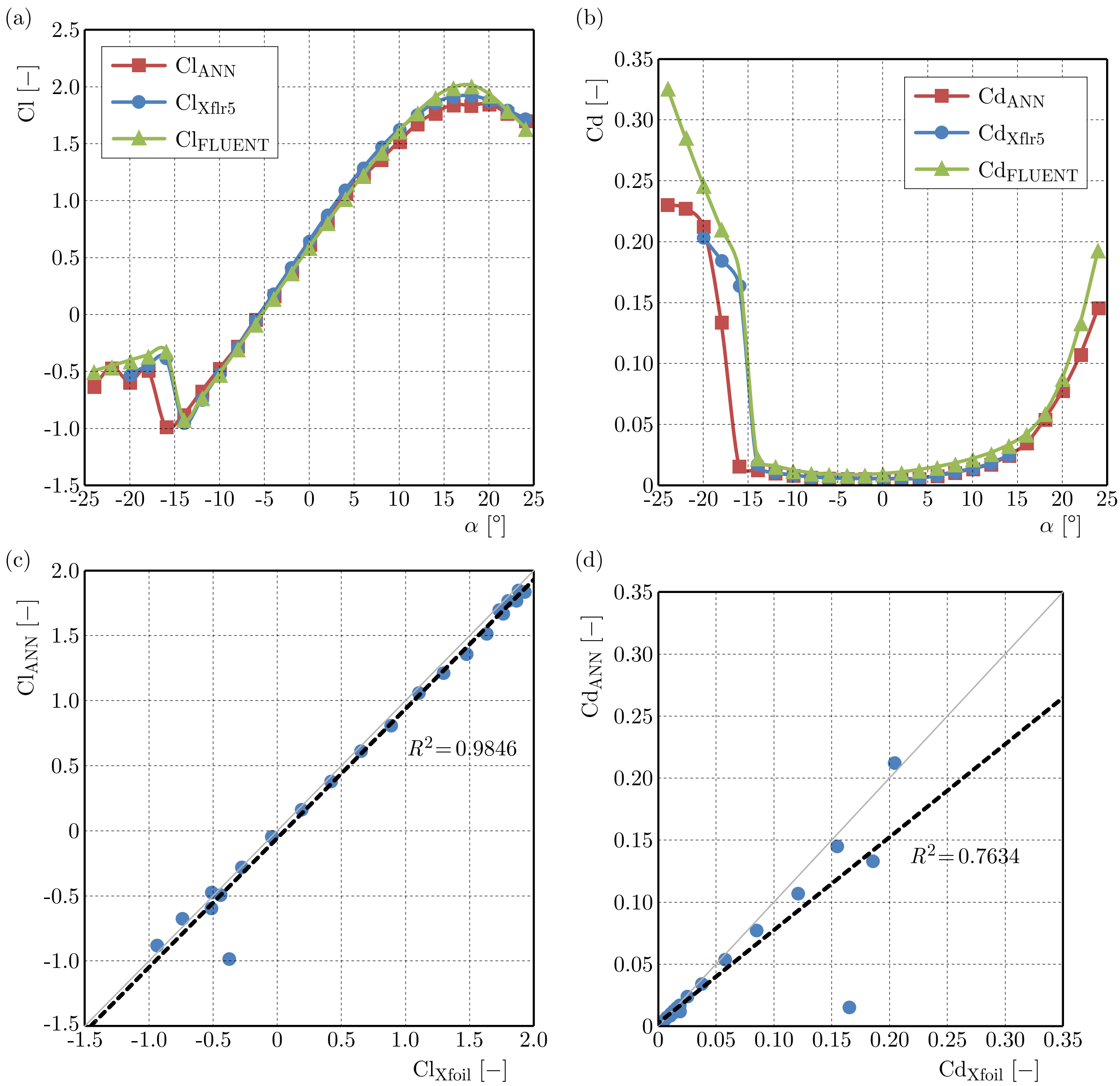

Fig. 11. Predicted by ANN and computed by Xfoil (Xflr5) lift (a) and drag (b) coefficients vs. the angle of attack, and the coefficient of determination of lift (c) and drag (d) coefficients for NACA (5.18)(4.18)12

A comparative analysis of the coefficient of determination of the lift and drag coefficients for all algorithms used was also performed. This comparison is shown in Fig. 13 with $\alpha = \pm 10°$.

The ANNs were trained on the data produced in Xfoil, which was the computational kernel of Xflr5, and therefore the predictions of the aerodynamic coefficients were consistent with the results calculated by Xfoil (Figs. 13a and 13b), and were characterised by $R^2 = 0.9995$ for C_l and $R^2 = 0.9983$ for C_d, respectively. In contrast, the coefficient of determination for the data predicted by the ANN and calculated in Ansys Fluent were $R^2 = 0.9980$ for C_l and $R^2 = 0.9657$ for C_d (Figs. 13e and 13f), respectively.

According to the references reviewed (Hsiao *et al.*, 2013; López-Briones *et al.*, 2020; Dhileep *et al.*, 2020) the lift coefficient calculated with Xfoil and Ansys Fluent were in agreement. This was confirmed by numerical tests, characterised by a coefficient of determination $R^2 = 0.9974$ (Fig. 13c). On the other hand, the frictional drag component was omitted from the Xfoil software and the aerodynamic drag coefficient was underestimated, with a coefficient of determination of $R^2 = 0.9652$ (Fig. 13d).

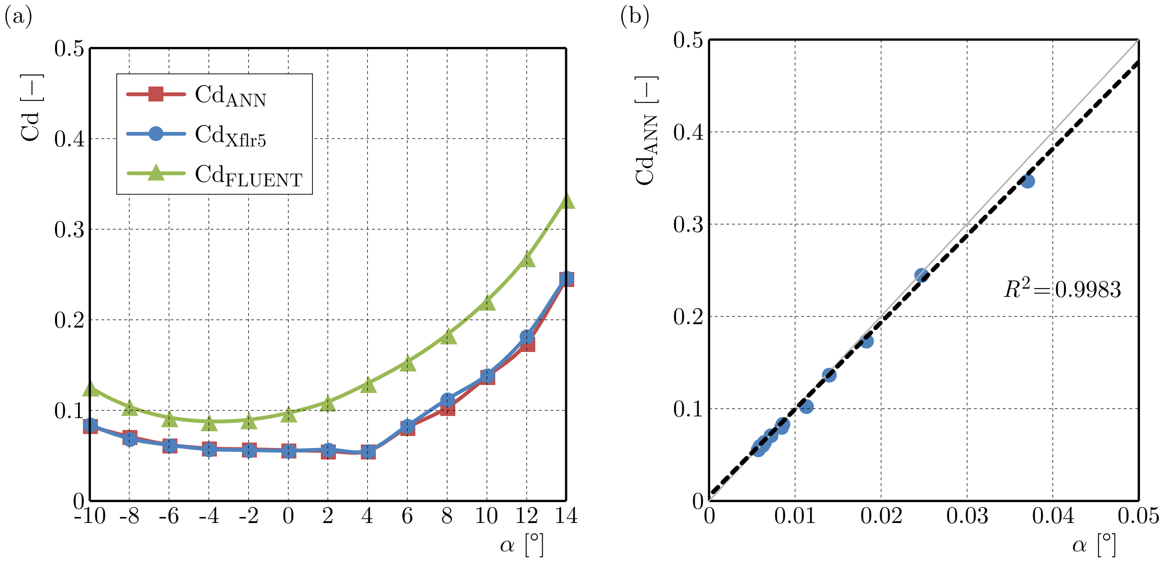

Fig. 12. Predicted by SSN and computed by Xfoil and FLUENT drag coefficient vs. the angle of attack (a) and coefficient of determination of the drag coefficient (b) for small angles of attacks ($-10 \leqslant \alpha \leqslant 16°$) for NACA (5.18)(4.18)12

The analyses were complemented by a comparison of the L/D ratio determined using the methods previously referred to (Fig. 14). The maximum L/D ratios determined by Xfoil and by ANN were $K_{max} = 197$ and $K_{max} = 195$, respectively, for the angle of attack $\alpha = 4°$. In contrast, due to inclusion of the frictional drag component in Ansys Fluent, the L/D ratio for the angle of attack $\alpha = 4°$ was much lower, $K = 78$. The maximum L/D ratio corresponded to the angle of attack $\alpha = 6°$ and was $K_{max} = 80$. The predicted excellence of the aerofoil calculated using Ansys Fluent decreased, as given in (Dhileep *et al.*, 2020).

5. Conclusion

This work demonstrates that the feed-forward artificial neural networks (FF-ANN) used to determine the lift and drag coefficients for a non-standard NACA four-digit aerofoil obtained the change in the lift coefficient as a function of the angle of attack, at a selected interval, with a coefficient of determination of $R^2 = 0.9846$, while for the drag coefficient, the change was a function of the angle of attack and $R^2 = 0.7634$ for the entire range of angles of attack tested. If the interval was narrowed to a range of $-10°$ to $+16°$, the coefficient increased to $R^2 = 0.9983$. The results obtained were compared to the experimental tests (Figs. 4a and 4b) for verification. The coefficient of determination for the lift coefficient, for angles of attack ranging from $-10°$ to $+16°$ was $R^2 = 0.9695$, which can be considered a good result. According to the knowledge from reference literature, the predicted aerofoil L/D ratio calculated using finite volumes decreased, relative to the panel method, but the nature of the L/D ratio change remained the same.

The disadvantages of the presented method are related to the disadvantages of metamodeling and machine learning. There are always errors in the metamodel due to interpolation of functions. In addition, when analyzing a different problem, or even the same problem but for a different Reynolds number, it is necessary to re-generate training data and train the SSN. Generalizing the algorithm for any Reynolds number would require a significant expansion of the database of training cases. In addition, the growth of the database would likely reduce the accuracy of prediction even for the Reynolds number found in the training case database. In further studies,

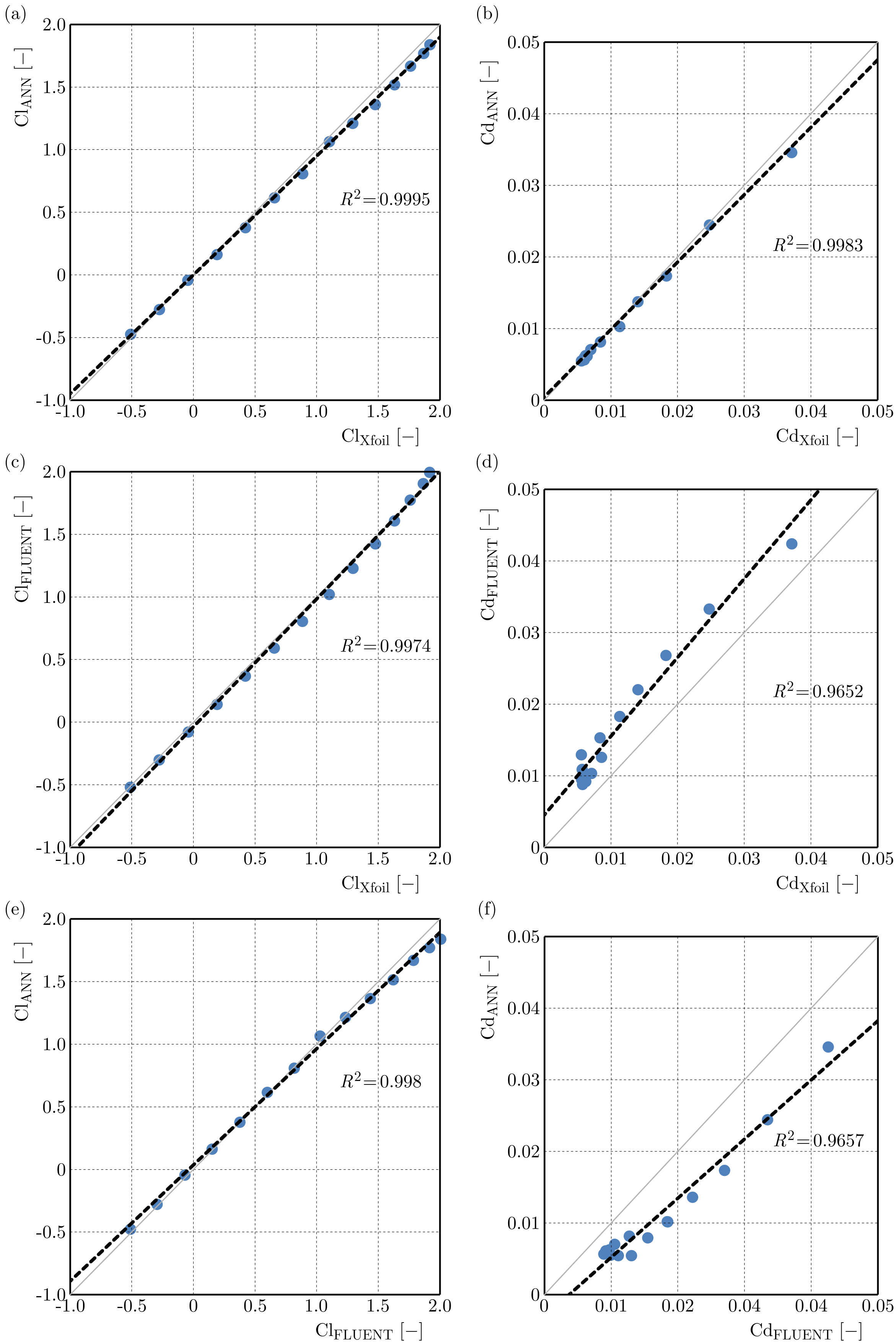

Fig. 13. Cross validation of coefficient of determination for lift (1st column) and drag (2nd column) coefficients (for $\alpha = \pm 10°$) for NACA (5.18)(4.18)12 calculated by ANN and Xfoil (a) and (b), FLUENT and Xfoil (c) and (d), ANN and FLUENT (e) and (f)

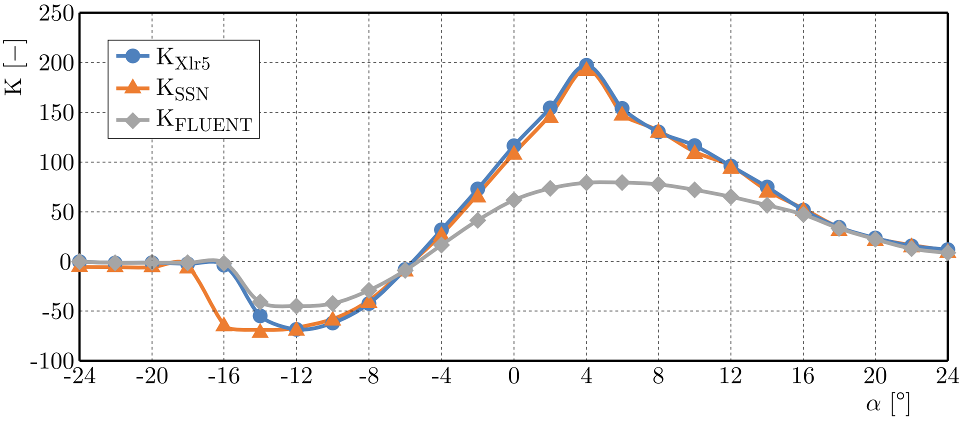

Fig. 14. Comparison of the L/D ratio determined with ANN, Xflr and Fluent

we intend to use finite volume methods (FVM) to obtain more accurate results by, among other things, taking into account frictional resistance, which Xfoil does not.

The proposed algorithm can be used as a metamodel for optimisation. The FF-ANNs reduced the execution time of the algorithm by replacing the solution of computer fluid mechanics equations (in the panel method), while retaining high accuracy for a properly selected range.

The optimised aerofoil will be used on the wing of an unmanned aerial platform designed under Project SZAFIR – Competition No. 4/SZAFIR/2021.

Acknowledgement

This paper was created as part of the project: Unmanned water surface/air platform using ground effect to support offshore Special Forces operations, funded by the NCBiR (National Centre for Research and Development), "SZAFIR" – Competition No. 4/SZAFIR/2021, Contract No. DOB--SZAFIR/01/B/036/04/2021 dated 20/12/2022.

References

1. Abbott H., Doenhoff E., Lous S., Stivers J., 1945, Summary of airfoil data, *National Advisory Commitee for Aeronautics Report*, **824**

2. Aramendia I., Fernandez-Gamiz U., Zulueta E., Saenz-Aguirre A., Teso-Fz-Betoño D., 2019, Parametric study of a Gurney flap implementation in a DU91W (2) 250 airfoil, *Energies*, **12**, 2, 294

3. Bakewell H.P., Lumley J.L., 1967, Viscous sublayer and adjacent wall region in turbulent pipe flow, *Physics Fluids*, **10**, 1880-1889

4. Berkooz G., Holmes P., Lumley J.L., 1993, The proper orthogonal decomposition in the analysis of turbulent flows, *Annual Review of Fluid Mechanics*, **25**, 539-575

5. Butterweck A., Głuch J., 2014, Neural network simulator's application to reference performance determination of turbine blading in the heat-flow diagnostics, [In:] *Intelligent Systems in Technical and Medical Diagnostics*, Springer, Berlin, Heidelberg

6. Conn A.R., Gould N.I. Toint P., 1991, A globally convergent augmented Lagrangian algorithm for optimization with general constraints and simple bounds, *SIAM Journal on Numerical Analysis*, **28**, 2, 545-572

7. Dhileep K., Kumar D., Ghosh S., Ali S.F., Arockiarajan A., 2020, Numerical study of camber morphing in NACA0012 airfoil, *Conference: AIAA AVIATION 2020 Forum*, 2781

8. Drela M., 1989, XFOIL: An analysis and design system for low Reynolds number airfoils, [In:] *Low Reynolds Number Aerodynamics. Proceedings of the Conference Noire Dame*, Indiana, USA, Springer Berlin Heidelberg, 1-12

9. Fukami K., Fukagata K., Taira K., 2021, Machine-learning-based spatio-temporal super resolution reconstruction of turbulent flows, *Journal of Fluid Mechanics*, **909**

10. Günel O., Ko E. Yavuz T. 2016, CFD vs. XFOIL of airfoil analysis at low Reynolds numbers, *IEEE International Conference on Renewable Energy Research and Applications (ICRERA)*, 628-632

11. Hsiao F.B., Bai C.J., Chong W.T., 2013, The performance test of three different horizontal axis wind turbine (HAWT) blade shapes using experimental and numerical methods, *Energies*, **6**, 6, 2784-2803

12. https://web.stanford.edu/ cantwell/AA200_Course_Material/The%20NACA%20airfoil %20series.pdf, [Online 2021.10.25]

13. Khan A.Y., Ahmad Z., Sultan T., Alshahrani S., Hayat K., Imran M., 2022, Optimization of photovoltaic panel array configurations to reduce lift force using genetic algorithm and CFD, *Energies*, **15**, 24, 9580

14. Kharal A., Saleem A., 2012, Neural networks based airfoil generation for a given Cp using Bezier-PARSEC parameterization, *Aerospace Science and Technology*, **23**, 1, 330-344

15. López-Briones Y.F., Sánchez-Rivera L.M., Arias-Montano A., 2020, Aerodynamic analysis for the mathematical model of a dual-system UAV, *17th International Conference on Electrical Engineering, Computing Science and Automatic Control (CCE)*

16. Oliveira R.F. de, 2021, https://github.com/theolivenbaum/XFOILinterface [Online 2021.12.02]

17. Porta Ko A., Smidt S., Schmehl R., Mandru M., 2023, Optimisation of a multi-element airfoil for a fixed-wing airborne wind energy system, *Energies*, **16**, 8, 3521

18. Saad M.M.M., Mohd S.B., Zulkafli M.F., Shibani W.M,, 2017, Numerical analysis for comparison of aerodynamic characteristics of six airfoils, *AIP Conference Proceedings*, AIP Publishing

19. San O., Maulik R., 2018, Neural network closures for nonlinear model order reduction, *Advances in Computational Mathematics*, **44**, 1717-1750

20. Sessarego M., Feng J., Ramos-García N., Horcas S.G., 2020, Design optimization of a curved wind turbine blade using neural networks and an aero-elastic vortex method under turbulent inflow, *Renewable Energy*, **146**, 1524-1535

21. Sekar V., Jiang Q., Shu, C., Khoo B.C., 2019, Fast flow field prediction over airfoils using deep learning approach, *Physics of Fluids*, **31**, 5, 057103

22. Sobieczky H., 1999, Parametric airfoils and wings, [In:] *Recent Development of Aerodynamic Design Methodologies*, Fujii K., Dulikravich G.S. (Edit.), Notes on Numerical Fluid Mechanics (NNFM), vol 65, Vieweg+Teubner Verlag

23. Sun G., Sun Y., Wang S., 2015, Artificial neural network based inverse design: Airfoils and wings, *Aerospace Science and Technology*, **42**, 415-428

24. Thirumalainambi R., Bardina J., 2003, Training data requirement for a neural network to predict aerodynamic coefficients, [In:] *Independent Component Analyses, Wavelets, and Neural Networks*, International Society for Optics and Photonics, 92-103

25. Verma N., Baloni B.D., 2021, Artificial neural network-based meta-models for predicting the aerodynamic characteristics of two-dimensional airfoils for small horizontal axis wind turbine, *Clean Technologies and Environmental Policy*, **24**, 2, 563-577

26. Viquerat J., Hachem E., 2020, A supervised neural network for drag prediction of arbitrary 2D shapes in laminar flows at low Reynolds number, *Computers and Fluids*, **210**, 104645

Manuscript received October 31, 2023; accepted for print January 13, 2024